Research Article | Vol. 10, No. 11 / 1 November 2019 / Biomedical Optics Express 5600
Biomedical Optics EXPRESS

Geometrical-optics approach to measure the optical density of bacterial cultures using a LED-based photometer

MASSIMILIANO LUCIDI,[1] MARCO MARSAN,[1] FRANCESCO PUDDA,[1] MATTIA PIROLO,[2] EMANUELA FRANGIPANI,[3] PAOLO VISCA,[2] AND GABRIELLA CINCOTTI[1,*]

[1]Engineering Department, University Roma Tre, via Vito Volterra 62, 00146 Rome, Italy
[2]Department of Science, University Roma Tre, viale Marconi 446, 00146 Rome, Italy
[3]Department of Biomolecular Sciences, University of Urbino Carlo Bo, Urbino, Italy
*gabriella.cincotti@uniroma3.it

Abstract: We develop a suitable geometrical-optics approach and demonstrate that it is possible to measure the optical density (OD) of bacterial cultures using a light emitting diode (LED)-based photometer. We measure both attenuation and spot-size variation, and we compensate for diffraction and stray-light impairment related to the incoherent source and large detection area. The approach is validated for different concentrations of two bacterial species, *Escherichia coli* and *Staphylococcus aureus*, that present different shapes and clustering organization.

1. Introduction

During the past decades, the number of infections and deaths caused by bacterial pathogens is steadily increasing in both developed and developing countries, where 1.8 million people are killed every year [1]. The presence of microorganisms significantly affects human health, and it is important to monitor bacterial concentration C (i.e. the number of cells per volume unit) not only in body fluids, but also in food, drugs and cosmetic products. There is a compelling need for novel, low-cost and rapid approaches to detect bacterial contamination in clinical, environmental, agri-food and industrial samples [2,3].

The development of new point of care testing (POCT) devices could drastically reduce the time and cost diagnosis, that can be performed in remote care centers, to monitor and reduce the spread of bacterial infections. Fast and accurate microbiological analysis of water and food is essential especially where resources are low, e.g., in low-income countries, in areas of military conflict or onboard ships. Hand-held devices are alternative solutions to conventional microbiological techniques to reduce the analysis complexity and cost [4]. Since bacteria multiply by binary division with very short generation times (20-40 min for common pathogens), measurement of bacterial growth in vitro is at the basis of most diagnostic procedures, and it is commonly used also in antimicrobial susceptibility testing.

A large variety of methods has been developed to evaluate microbial concentration, measuring the cell number, mass, or constituents. The two most widely used approaches to determine the bacterial concentration C are the viable plate count, that measures the colony forming unit per milliliter (CFU/ml), and the spectrophotometry, that determines the optical density (OD) of a liquid sample. The plate count enumerates the bacterial colonies grown on a (selective) nutrient medium, that become visible to the naked eye after 24-72 hours of incubation at a target temperature. The laboratory procedure involves making serial dilutions of the sample with sterile saline solution, to ensure that a suitable number of viable bacterial cells, hence colonies, are generated. Even though the approach is highly sensitive (in theory, a single cell develops a colony, therefore the number of colonies detected directly correlates with the number of viable cells), the

#371994 https://doi.org/10.1364/BOE.10.005600
Journal © 2019 Received 5 Jul 2019; revised 9 Sep 2019; accepted 2 Oct 2019; published 8 Oct 2019

Biomedical Optics EXPRESS

method presents some disadvantages, since only living and culturable bacterial cells generate colonies, and it is also possible that cluster of cells develop into a single colony.

The spectrophotometric approach correlates the cell concentration C in a pure culture with the scattered light, and presents inherent advantages of being rapid and nondestructive [5]. Nowadays, the OD values have become synonymous with bacterial concentration [6] and the relation with CFU/ml measurements strictly depends on the bacterial species and on their growth condition [7,8].

A spectrophotometer measures the turbidity of a liquid sample, originated by suspended insoluble particles [9,10]. According to the Beer-Lambert law, the OD parameter, or absorbance A is measured as a function of the attenuation α that a collimated light beam undergoes when propagating along a known distance h through the medium

$$\frac{\Phi_t}{\Phi_i} = 10^{-A} = e^{-\alpha h}. \tag{1}$$

Φ_t and Φ_i are the intensities transmitted through the sample and the reference liquid (*blank*), respectively. In a homogeneous solution, the absorbance A is proportional to the solute concentration; on the other hand, in suspensions, such as bacterial cultures, the amount of light reaching the detector is further reduced due to the scattering process, and the overall attenuation parameter $\alpha = \sigma \cdot C$ is proportional to the particle concentration C [6]. The scattering cross section σ depends on the shape and size of the particles [11] and when particle concentration C becomes high, multiple scattering events may strongly affect the measurement results [12–15]. Finally, bacteria often present a planktonic behavior and the liquid can be considered as a suspension of dispersed bacterial cells; however, depending on the method of inoculation, some bacterial species tend to generate aggregates or clusters [16]. For all these reasons, the accuracy of the spectrophotometric measurement is often limited, and it strongly depends on both instrument configuration and biological sample.

Most commercial bench-top spectrophotometers available in laboratories and medical facilities use coherent sources, such as laser and monochromators, as well as photodetectors or photomultiplier tubes. The sample is illuminated by a beam of parallel, monochromatic light rays, propagating along a direction perpendicular to the sample surface. The light travels for a length h inside the liquid and the intensity is reduced to Φ_t, due to the number of cells encountered along the light path, that scatter and attenuate the beam.

The replacement of the laser or the monochromator with a LED source would simplify the optical architecture and reduce the device cost, that are key requirements for POCT devices. However, to the best of our knowledge, LED-based spectrophotometers have not been proposed yet to measure the OD parameter, because their accuracy is hampered by stray-light effects. In fact, LED emits an incoherent and not collimated beam, and each ray propagates for a different length inside the sample and undergoes a different attenuation and scattering process.

In the present paper, we use a LED-based photometer and develop a suitable geometrical-optics approach to increase the accuracy of OD measurements. The device architecture shown in Fig. 1(a) is ideal for POCT, and consists of a LED, a lens and a complementary metal-oxide semiconductor (CMOS) sensor. In a recent work, we have used the same photometer to measure both concentration and refractive index of a homogenous liquid [17]. We now use this general-purpose POCT device to measure the OD of microbiological suspensions. To enhance the measurement accuracy and compensate for stray-light effects, we have developed a simple, but effective, geometrical-optics model to describe the propagation of coherent and incoherent optical beams through a scattering medium, based on the Fokker-Planck equation. We demonstrate that by multiplying the attenuation parameter measured with the POCT sensor by a factor of 3, accurate OD measurements of bacterial specimens can be obtained, that are comparable with bench-top expensive spectrophotometers.

Biomedical Optics EXPRESS

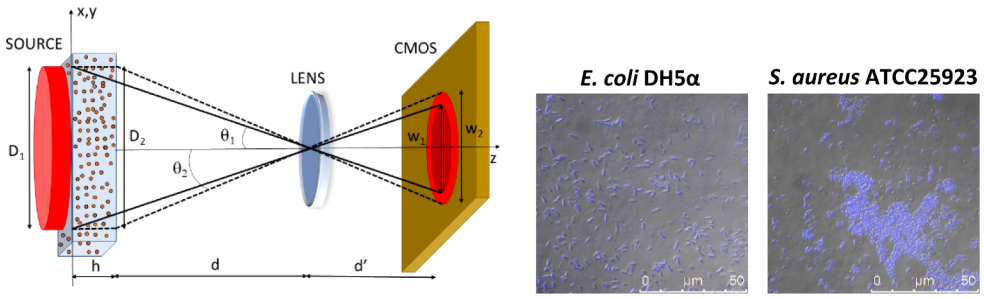

Fig. 1. (a) Spectrophotometer layout (drawing not in scale). (b) Confocal microscopy images of *E. coli* DH5α and *S. aureus* ATCC25923. Merged differential interference contrast (DIC) and DAPI images.

The POCT device can be used to measure the concentration of a solute, such as a dye, in a homogenous liquid. In this case, the spot size of the beam transmitted through the liquid sample, does not change with the solute concentration, but it depends on the liquid under examination [17]. In the present work, we use the same low-cost LED-based sensor to measure the OD of a turbid liquid, such as a bacterial suspension. In this case, the beam spot size increases with the number of bacterial cells due to scattering effects. The spot-size enlargement can be evaluated using the Fokker-Planck equation, and the model fits with the measured values.

2. Methods

2.1. Bacterial specimens

Since size and shape highly influence the OD measurements [11], we consider two different bacterial species: Gram-negative, rod-shaped *Escherichia coli* (*E. coli*) (strain DH5α) and Gram-positive, round-shaped conglomerates-grape-like clusters-forming *Staphylococcus aureus* (*S. aureus*) (strain ATCC25923). The average radius of *S. aureus* (0.4 μm) and the average length and diameter of *E. coli* (1.6 μm and 0.9 μm, respectively) have been measured on individual stationary-phase cells by laser scanning confocal microscopy; these values are in agreement with literature data [11,18].

To obtain a bacterial population prevalently composed of single cells, about four bacterial colonies were picked from a fresh Tryptic Soy Agar (TSA) plate, suspended in Tryptic Soy Broth and incubated at 37°C for 18 hours, until the stationary phase was reached. Then, bacterial suspensions were centrifuged at 5,000 rpm for 5 minutes to harvest the cells, that were resuspended in 0.9% *NaCl* solution (saline solution from now on) to reach a final value OD_{600}=1, measured using the commercial photometer *BioPhotometer basic Eppendorf* at 600 nm wavelength. These *E. coli* and *S. aureus* stationary cultures have been also imaged using a laser scanning confocal microscope, to ensure that the population was prevalently composed by individual cells. The number of cells in the bacterial cultures have been also measured by evaluating the viable counts on TSA plates. The CFU/ml are 2.25 10^8 (+/− 5.45 10^7) and 3.50 10^8 (+/− 3.16 10^7) for *E. coli* DH5α and *S. aureus* ATCC25923, respectively.

Finally, bacterial cultures were further diluted with sterile saline solution, and five two-fold serial dilutions were performed to obtain the samples to be measured. The number of cells in the diluted bacterial cultures are reduced proportionally to the dilution ratio.

Figure 1(b) shows the images of the bacterial species acquired by laser scanning confocal microscope. In this case, *E. coli* and *S. aureus* were stained adding 1 μg/ml 4',6-diamidino-2-phenylindole (DAPI) blue fluorescent dye directly on the bacterial culture and lied on a slide glass

Biomedical Optics EXPRESS

covered with agarose 0.5%. The bacterial samples were visualized using a Leica SP5 confocal laser-scanning microscope equipped with a 63× oil immersion objective. From an inspection of Fig. 1(b), it is evident that the two bacterial species present cells with different shape and clustering organization.

2.2. Measurement setup

OD measurements were obtained at λ=600 nm reference wavelength (OD_{600}) using polystyrene cuvettes (*2xOptical, Sarstedt*) with $h = 10$ mm optical path length, filled with 3 ml of bacterial suspension. For each sample, the OD value was measured using the LED-based sensor and the commercial spectrophotometers *BioPhotometer basic Eppendorf* (considered as the reference) and *BioPhotometer Spectrophotometer UV/VIS Eppendorf*. In addition, the OD parameter was also measured using two microplate readers *Wallac 1420 Victor3 V PerkinElmer* and *Tecan Spark*. In this case, 100 μl of the bacterial suspension has been inserted in each well of a polystyrene 96-well flat-base microtiter plate (*Sarstedt*). Since the optical path travelled by the optical beam is different in these two reader platforms, we used fixed scaling factors of 11.84 and 5.29 for the microplate readers *Wallac 1420 Victor3 V PerkinElmer* and *Tecan Spark*, respectively. In this way, the optical path difference has been compensated and all the OD values can be compared.

2.3. POCT sensor

The low-cost, portable POCT sensor (*WeLab*, *DNAPhone*) mounts a LED source (*Flora* RGB *Smart NeoPixel* version 2, *Adafruit*), a 5 Megapixel CMOS sensor (*OmniVision* OV5647, *OmniBSI*) (*Raspberry Pi* Camera) and a lens [19]. The device has the optical architecture illustrated in Fig. 1 (a). The LED is followed by a diffuser and a pinhole, and in Fig. 1(a) the source is schematically modelled as an incoherent disk with diameter $D_1 = 4$ mm, at a distance d from the lens, with angular aperture $\theta_1 = \text{atan}(D_1/2d) = 4.52$ deg [17]. The emission range of red light is 620-630nm, with intensity 550-700 mcd. The lens has focal length $f = 3.6$ mm and f-number $f/2.9$, and it is placed at a distance d' from the CMOS sensor.

For each measurement, an 8-bit 800 × 800 pixels raw image is acquired, using only red-light source, to obtain data compatible with conventional OD_{600}. The OD parameter A of Eq. (1) is measured as function the average intensities Φ_i and Φ_t transmitted through the sample and the *blank*, respectively, evaluated over a circular sensor area of diameter 540 pixels, using Eq. (4) of Ref. [17].

We assume that the intensity distribution of the radiation emitted by the incoherent disk has a Gaussian profile, with full spot-size D_1=4mm, and that its image on the camera has a dimension w_1=0.4 mm (magnification factor $M = d'/d = 0.1$) [17]. When a cuvette filled with saline solution (*blank*) is placed in the beam lightpath, the spot size w_2 measured on the CMOS sensor increases due to light refraction. In the case that bacterial cells are present in the sample, the measured spot size further increases due to cell scattering, and it depends of the OD parameter, i.e. the cell concentration C.

In all the experiments, the beam spot size is measured as the round area on the CMOS sensor covered by the 8-bit pixels (value range 0-255) with values larger than $R = e^{-1}*2^8$=0.37*255~94 [17].

2.4. Geometrical-optics model

We refer to the Wigner distribution $W(\boldsymbol{r},\boldsymbol{k},z)$, that describes the light field at the plane $z = const.$ as a density of 'rays' with lateral velocity $c\boldsymbol{k}(k_x, k_y)/k_0$ and lateral position $\boldsymbol{r}(x,y)$; c is the light speed in vacuum, $\boldsymbol{k}(k_x, k_y)$ the wavevector, and k_0 the wavenumber [20].

The beam propagation inside a bacterial suspension can be modelled as a series of scattering events, each of them slightly changes the direction $\boldsymbol{k}(k_x, k_y)$ of ray propagation. In the continuous

Biomedical Optics EXPRESS

limit of an infinitely small distance between two consecutive scattering events, the field propagation can be described by the Fokker-Planck equation [21]

$$\frac{\partial W(\boldsymbol{r},\boldsymbol{k},z)}{\partial z}+\frac{k_x}{k_0}\frac{\partial W(\boldsymbol{r},\boldsymbol{k},z)}{\partial x}+\frac{k_y}{k_0}\frac{\partial W(\boldsymbol{r},\boldsymbol{k},z)}{\partial y}=qk_0^2\left(\frac{\partial^2 W(\boldsymbol{r},\boldsymbol{k},z)}{\partial^2 k_x}+\frac{\partial^2 W(\boldsymbol{r},\boldsymbol{k},z)}{\partial^2 k_y}\right), \quad (2)$$

where the change of the propagation direction depends on the scattering strength parameter q. The q parameter is a measure of the medium scattering strength and is linearly proportional to the cell concentration C, in the single-scattering regime.

The left-hand side terms in Eq. (2) correspond to the transport equation in a homogeneous medium ($q=0$): in this case, the solution of Eq. (2) has the form [20]

$$W(\boldsymbol{r},\boldsymbol{k},z)=W\left(\boldsymbol{r}-\frac{\boldsymbol{k}}{k_0}z,\boldsymbol{k},0\right). \quad (3)$$

Therefore, if a single ray propagates through an homogenous medium with refractive index n, its direction $\boldsymbol{k}(k_x,k_y)$ remains the same, and its position $\boldsymbol{r}(x,y)$ changes of $z\boldsymbol{k}/k_0 = z\,n\sin\theta_1$. Therefore, the ray displacement, and the corresponding spot-size increase, due to light refraction can be used to determine the liquid refractive index n [17].

If the field distribution at the $z=0$ plane is known, the field transmitted in the turbid medium can be evaluated as [22]

$$\begin{aligned} W(\boldsymbol{r},\boldsymbol{k},z) &= \frac{3}{4\pi^2 q^2 k_o^2 z^4} \\ &\times\int\int W(\boldsymbol{r}',\boldsymbol{k}',0)e^{-\frac{3}{qz^3}\left(\left|\boldsymbol{r}-\boldsymbol{r}'-\frac{\boldsymbol{k}'}{k_0}z\right|^2-\frac{z}{k_0}(\boldsymbol{k}-\boldsymbol{k}')\cdot\left(\boldsymbol{r}-\boldsymbol{r}'-\frac{\boldsymbol{k}'}{k_0}z\right)+\frac{z^2}{3k_0^2}|\boldsymbol{k}-\boldsymbol{k}'|^2\right)}d^2\boldsymbol{r}'d^2\boldsymbol{k}' \\ &=\int\int W(\boldsymbol{r}',\boldsymbol{k}',0)K_k(\boldsymbol{k}-\boldsymbol{k}')K_r\left(\boldsymbol{r}-\boldsymbol{r}'-\frac{\boldsymbol{k}+\boldsymbol{k}'}{2k_0}z\right)d^2\boldsymbol{r}'d^2\boldsymbol{k}'. \end{aligned} \quad (4)$$

We have written the propagation kernel as the product of two *ray-spread functions* [20]

$$K_k(\boldsymbol{k}-\boldsymbol{k}')=\frac{1}{4\pi qzk_o^2}e^{-\frac{|\boldsymbol{k}-\boldsymbol{k}'|^2}{4qzk_0^2}} \quad (5)$$

$$K_r\left(\boldsymbol{r}-\boldsymbol{r}'-\frac{\boldsymbol{k}+\boldsymbol{k}'}{2k_0}z\right)=\frac{3}{\pi qz^3}e^{-\frac{3}{qz^3}\left|\boldsymbol{r}-\boldsymbol{r}'-\frac{\boldsymbol{k}+\boldsymbol{k}'}{2k_0}z\right|^2} \quad (6)$$

that measure the change of the ray direction $\boldsymbol{k}(k_x,k_y)$ and ray position $\boldsymbol{r}(x,y)$ due to the scattering, respectively; in the limit that q goes to 0, both functions become a Dirac delta.

We observe that ray direction changes with variance $2qz$ (Eq. (5)), whereas the variation of the ray position (**r**-**r**') has an average value ($\boldsymbol{k}+\boldsymbol{k}$')/2 and variance $qz^3/6$ (Eq. (6)).

At this point, we can relate the OD parameter, or absorbance $A=\alpha h/ln(10)=0.43\alpha h$, to the scattering strength q. According to the van de Hulst's scattering model [10], when illuminated by a coherent plane wave travelling in the z direction, each particle generates a spherical wave, and, in the paraxial approximation, the forward travelling wave is attenuated as in Eq. (1). The beam attenuation is equal to *radiant emittance*, and in the paraxial approximation it is [20]

$$e^{-\alpha h}=1-\alpha h=1-\frac{\langle|\boldsymbol{k}|^2\rangle}{2k_o^2}=1-\frac{1}{2k_o^2}\frac{\int|\boldsymbol{k}|^2W(\boldsymbol{r},\boldsymbol{k},z=h)d^2\boldsymbol{k}}{\int W(\boldsymbol{r},\boldsymbol{k},z=h)d^2\boldsymbol{k}}. \quad (7)$$

We separately analyze the cases when the source radiation is coherent and spatially incoherent. The first case embodies the light emitted by a laser or at the output of a monochromator, as in commercial bench-top spectrophotometers, or multi-plate readers. On the other hand, the LED of the POCT photometer can be modelled as an incoherent source.

Biomedical Optics EXPRESS

2.5. Coherent source

We refer to a monochromatic plane wave, with uniform intensity distribution, that is described by the Wigner function at the $z = 0$ plane

$$W(\boldsymbol{r}, \boldsymbol{k}, 0) = \Phi_1 \delta(\boldsymbol{k}), \tag{8}$$

where Φ_1 is the average intensity and $\delta(\boldsymbol{k})$ the Dirac delta. Substituting into Eq. (4), we obtain

$$W(\boldsymbol{r}, \boldsymbol{k}, z = h) = \frac{\Phi_1}{4\pi q h k_0^2} e^{-\frac{|\boldsymbol{k}|^2}{4qhk_0^2}}. \tag{9}$$

In this case, all the rays travel the cuvette along the z axis, and they are scattered along directions $\boldsymbol{k} \neq 0$. The scattered light does not reach the detector and the measured beam absorbance is proportional to the average angular spread $\alpha h = 2qh$. Substituting Eq. (9) into Eq. (7), we relate the OD parameter $A = 0.43\alpha h = 0.86qh$ to the scattering strength q [22]. As expected, the scattering parameter q (*i.e*, the number of bacterial cells inside the liquid) is proportional to the OD.

2.6. Incoherent source

In the case of an incoherent source, the Wigner distribution at the $z = 0$ plane does not depend on $\boldsymbol{k}(k_x, \mathrm{k_y})$ and coincides with the beam intensity profile $W(\mathbf{r}, \mathbf{k}, 0) = \Phi(\mathbf{r})$. In this case, Eq. (4) becomes

$$W(\boldsymbol{r}, \boldsymbol{k}, z) = \frac{3}{4\pi q z^3} \int \Phi(\boldsymbol{r}') e^{-\frac{3}{4qz^3}\left|\boldsymbol{r}-\boldsymbol{r}'-\frac{\boldsymbol{k}}{k_0}z\right|^2} d^2\boldsymbol{r}', \tag{10}$$

and the angular spread is $2qz/3$. The source light is described by rays propagating along all the directions $\boldsymbol{k}(k_x, \mathrm{k_y})$, each of them undergoes to scattering events described by Eq. (5). From an inspection of Eq. (10), it is also evident that the spatial coherence increases in propagation, according to the van Cittert- Zernike theorem.

We have obtained the main result of this work, and demonstrate that for any incoherent source with arbitrary intensity profile, the OD parameter $A = 0.43\alpha h = 0.43 \cdot 2qh/3 = 0.29\ q\ h$ is still linearly proportional to the scattering strength q. However, for a given bacterial concentration, the OD measured with a coherent source is three times the absorbance measured with an incoherent LED.

In the POCT photometer, the LED followed by a diffuser and a pinhole is an incoherent disk with diameter $D_1 = 4$ mm and angular aperture $\theta_1 = \mathrm{atan}(D_1/2d) = 4.52$ deg. We model the intensity distribution at the source plane $\Phi(\boldsymbol{r})$ with a Gaussian profile with full spot-size D_1 [17] and the corresponding Wigner distribution function is

$$W(\boldsymbol{r}, \boldsymbol{k}, 0) = \Phi(\boldsymbol{r}) = \frac{4\Phi_1}{\pi D_1^2} e^{-4\frac{|\boldsymbol{r}|^2}{D_1^2}}. \tag{11}$$

The lens makes an image on the CMOS sensor with full spot-size $w_1 = M \cdot D_1 = 0.4$ mm ($M = 0.1$ magnification parameter).

If the light beam is transmitted through a cuvette filled with saline solution (*blank*), the beam full spot-size D_2 increases due to ray displacement related to the presence of the liquid (Snell's

Biomedical Optics EXPRESS

law), and the average intensity Φ_2 slightly decreases due to the liquid absorbance [17]

$$\Phi_i(\boldsymbol{r}) = \frac{4\Phi_2}{\pi D_2^2} e^{-4\frac{|\boldsymbol{r}|^2}{D_2^2}}. \tag{12}$$

$D_2 = 2.84$ mm is evaluated as a function of the corresponding image full spot size w_2=$d'D_2/(d-h) = 0.47$ mm, and $\theta_2 = \text{atan}(w_2/2d') = 5.31$ deg. Inserting Eq. (12) in Eq. (10), we obtain

$$W(\boldsymbol{r}, \boldsymbol{k}, z) = \frac{4\Phi_2}{\pi D^2(z)} e^{-4\frac{\left(r - \frac{\boldsymbol{k}}{k_0} z\right)^2}{D^2(z)}}, \tag{13}$$

that is solution of Eq. (2) if

$$D^2(z) = D_2^2 + \frac{16}{3} q z^3. \tag{14}$$

Therefore, the spot size of the beam propagated through a bacterial solution enlarges as a function of the absorbance A

$$D^2(h) = D_2^2 + \frac{16}{3 \cdot 0.29} A \cdot h^2 = D_2^2 + 18.4\, A \cdot h^2. \tag{15}$$

and the overall beam dimension can be evaluated as the ratio between the spot-size and the average angular spread (from Eq. (7))

$$\frac{D(h)}{\frac{\langle |\boldsymbol{k}|^2 \rangle}{k_o^2}} = \frac{\sqrt{D_2^2 + 18.4\, A \cdot h^2}}{2 - e^{-\alpha h/2}} = \frac{\sqrt{D_2^2 + 18.4\, A \cdot h^2}}{2 - e^{-1.16\, A}}. \tag{16}$$

3. Results

Figure 2 reports the raw images of the light beam transmitted directly, without introducing a cuvette in the device, through a saline solution (blank) and through four different concentrations of the *S. aureus* culture. The corresponding axial beam profiles are plotted in Fig. 3. From an inspection of Fig. 3(a), it is evident that the maximum beam intensity decreases with the bacterial concentration; on the other hand, the normalized beam profiles of Fig. 3(b) confirm that the beam spot-size w_2 increases with the number of cells. The beam spot-size is measured as the sensor area (approximated to a circle) covered by the 8-bit pixels with normalized values larger than R = 94 [17], and it is plotted in Fig. 4, where red (blue) diamonds refer to measured values for *E. coli* (*S. aureus*) cultures, respectively.

Figure 4 reports also the line corresponding to the model of Eq. (16). In a homogeneous liquid the beam spot-size does not change with the solute concentration, and it can be used to measure the liquid refractive index [17]. On the other hand, in a turbid liquid, such as a bacterial suspension, the beam spot-size increases with the number of cells. Therefore, accurate cell concentration measurements can be achieved measuring both spot-size enlargement and beam attenuation.

The bacterial cell size and shape can be determined measuring attenuation and angular scattering, using the Gaussian ray approximation of anomalous diffraction [11]. However, in our measurements based on incoherent light, we measured similar spot-size values for *S. aureus* and *E. coli*.

Figure 5 reports the OD measurements obtained with the LED-based photometer considering the sensor areas of diameter 540 pixels, and evaluating the absorbance parameter using Eq. (4) of Ref. [17]. We observe that if we multiply the measured value for a factor 3, the accuracy of the OD measurements in the range [0.1-1.5], obtained with the LED-based photometer is

Biomedical Optics EXPRESS

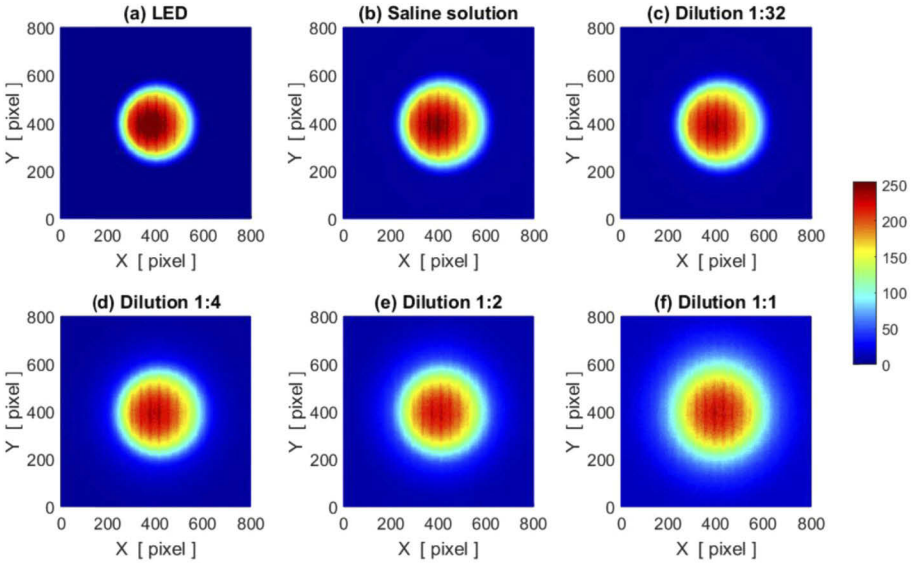

Fig. 2. Artificial-color rendering of raw images for *S. aureus* bacterial suspension at different concentrations. (a) without cuvette; (b) saline solution (*blank*); (c) bacterial suspension at dilution ratios of 1:32; (d) 1:4; (e) 1:2; (f) 1:1.

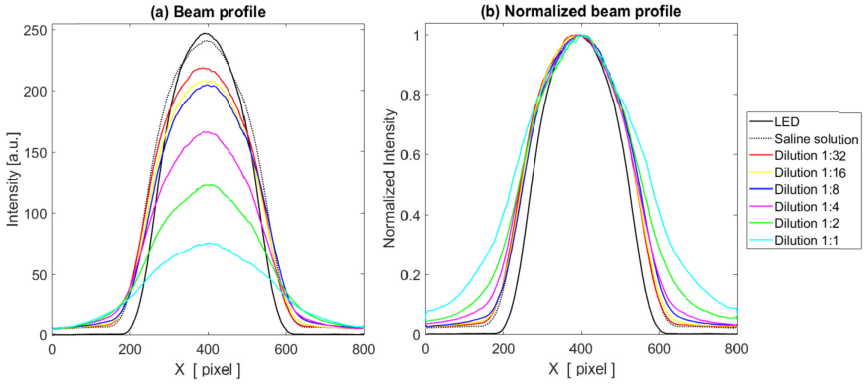

Fig. 3. (a) Axial beam profiles. (b) Axial beam profiles normalized to their own maxima. Data have been smoothed with a moving-average filter only for plot rendering. It is evident that, due to the scattering process, the spot-size increases with the number of cells.

Biomedical Optics EXPRESS

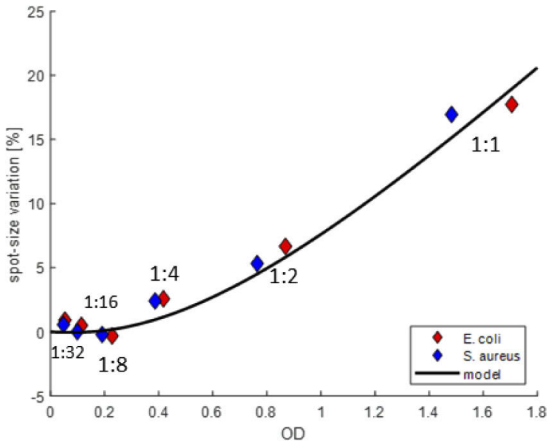

Fig. 4. Beam spot-size variation versus OD parameter measured with the reference spectrophotometer *BioPhotometer basic*. Red (blue) diamonds refer to measured values for *E. coli* (*S. aureus*) cultures, and the black line represents the model of Eq. (16).

similar to that of commercially available bench-top spectrophotometers and multi-well readers [23]. Therefore, using the existing optical architecture, the detection limit is about OD = 1.5, but it could be further increased reducing the distances *d* and *d*', as well using a more intense LED source.

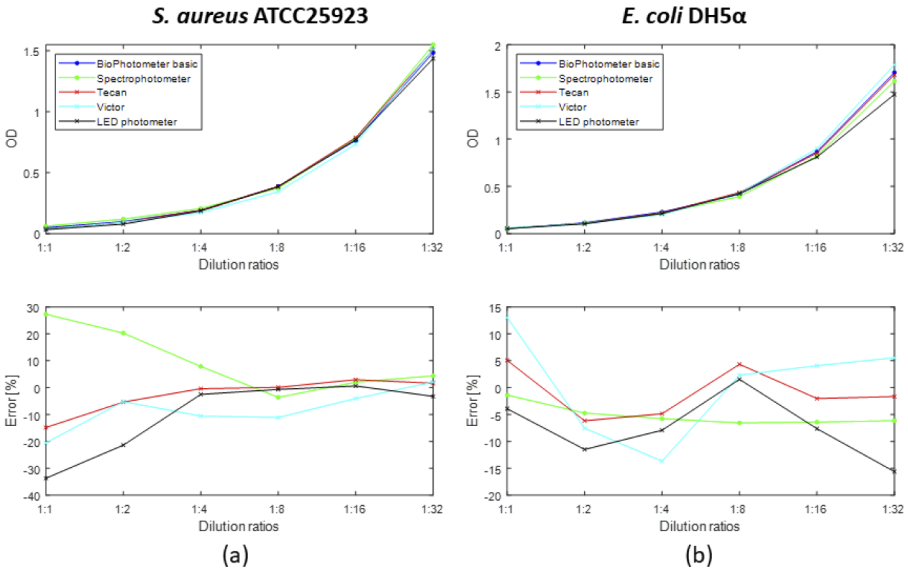

Fig. 5. OD measurements (and relative errors) of (a) *S. aureus* ATCC25923 and (b) *E. coli* DH5α bacterial suspensions, obtained with the LED-based photometer, two commercial spectrophotometers and two multi-label plate readers. The errors have been evaluated with respect to the OD values obtained with the reference spectrophotometer *BioPhotometer basic*.

Biomedical Optics EXPRESS

Summary

We have developed an accurate geometrical-optics model to evaluate the scattering effect using an incoherent light emitted from a LED source, and we have demonstrated that the average beam angular spread is a third of the value corresponding to a coherent beam. Therefore, if we multiply the attenuation parameter for a constant equal to 3, we can obtain accurate OD measurements of bacterial specimens, using an inexpensive portable POCT device. The photometer has a do-it-yourself (DIY) architecture, to allow everybody to fabricate a customized low-cost sensor, for different microbiological analysis.

Funding

Regione Lazio (A0114-2017-14829, A0114E0030, MBSMART, POR FESR LAZIO 2014 – 2020).

Acknowledgments

The Authors are grateful to Dr. Alessandro Candiani and DNAPhone for their support and assistance. We are also thankful to anonymous Reviewers whose comments helped us to improve the technical quality of the paper.

Disclosures

The Authors declare that there are no conflicts of interest related to this article.

References

1. J. de Dieu Habimana, J. Ji, and X. Sun, "Minireview: trends in optical-based biosensors for point-of-care bacterial pathogen detection for food safety and clinical diagnostics," Anal. Lett. **51**(18), 2933–2966 (2018).
2. M. Drancourta, A. Michel-Lepagea, S. Boyerb, and D. Raoulta, "The point-of-care laboratory in clinical microbiology," Clin. Microbiol. Rev. **29**(3), 429–447 (2016).
3. M. Grossi, C. Parolin, B. Vitali, and B. Riccò, "Measurement of bacterial concentration using a portable sensor system with a combined electrical-optical approach," to appear in IEEE Sens. J.
4. M. Safavieh, M. Ahmed, E. Sokullu, A. Ng, L. Braescu, and M. Zourob, "A simple cassette as point-of-care diagnostic device for naked-eye colorimetric bacteria detection," Analyst **139**(2), 482–487 (2014).
5. A. L. Koch, "Turbidity measurements of bacterial cultures in some available commercial instruments," Anal. Biochem. **38**(1), 252–259 (1970).
6. K. Stevenson, A. F. McVey, I. B. Clark, P. S. Swain, and T. Pilizota, "General calibration of microbial growth in microplate readers," Sci. Rep. **6**(1), 38828 (2016).
7. S. Clais, G. Boulet, M. Van kerckhoven, E. Lanckacker, P. Delputte, L. Maes, and P. Cos, "Comparison of viable plate count, turbidity measurement and real-time PCR for quantification of Porphyromonas gingivalis," Lett. Appl. Microbiol. **60**(1), 79–84 (2015).
8. H.-L. Lin, C.-C. Lin, Y.-J. Lin, H.-C. Lin, C.-M. Shih, C.-R. Chen, R.-N. Huang, and T.-C. Kuo, "Revisiting with a relative-density calibration approach the determination of growth rates of microorganisms by use of optical density data from liquid cultures," Appl. Environ. Microbiol. **76**(5), 1683–1685 (2010).
9. S. E. Harding, "Applications of light scattering in microbiology," Biotechnol. Appl. Biochem. **8**(6), 489–509 (1986).
10. H. C. Van De Hulst, *Light Scattering by Small Particles* (Dover, 1953).
11. A. Katz, A. Alimova, M. Xu, E. Rudolph, M. K. Shah, H. E. Savage, R. B. Rosen, S. A. McCormick, and R. R. Alfano, "Bacteria size determination by elastic light scattering," IEEE J. Sel. Top. Quantum Electron. **9**(2), 277–287 (2003).
12. L. Wind and W. W. Szymanski, "Quantification of scattering corrections to the Beer-Lambert law for transmittance measurements in turbid media," Meas. Sci. Technol. **13**(3), 270–275 (2002).
13. J. V. Lawrence and S. Maier, "Correction for the inherent error in optical density readings," Appl. Environ. Microbiol. **33**(2), 482–484 (1977).
14. A. Meyers, C. Furtmann, and J. Jose, "Direct optical density determination of bacterial cultures in microplates for high-throughput screening applications," Enzyme Microb. Technol. **118**, 1–5 (2018).
15. X. Sun, X. Li, and L. Ma, "A closed-form method for calculating the angular distribution of multiply scattered photons through isotropic turbid slabs," Opt. Express **19**(24), 23932–23937 (2011).
16. K. N. Kragh, M. Alhede, M. Rybtke, C. Stavnsberg, PØ Jensen, T. Tolker-Nielsen, M. Whiteley, and T. Bjarnsholt, "Inoculation method could impact the outcome of microbiological experiments," Appl. Environ. Microbiol. **84**(5), e02264 (2017).

Biomedical Optics EXPRESS

17. M. Marsan, M. Lucidi, F. Pudda, M. Pirolo, E. Frangipani, P. Visca, and G. Cincotti, "A geometrical-optics approach to increase the accuracy in LED-based photometers for point-of-care testing," Biomed. Opt. Express **10**(7), 3654–3662 (2019).
18. J. Schwarz-Linek, J. Arlt, A. Jepson, A. Dawson, T. Vissers, D. Miroli, T. Pilizota, V. A. Martinez, and W. C. K. Poon, "Escherichia coli as a model active colloid: A practical introduction," Colloids Surf., B **137**, 2–16 (2016).
19. https://www.we-lab.it/en/welabmaker
20. M. J. Bastiaans, "Application of the Wigner distribution function to partially coherent light," J. Opt. Soc. Am. A **3**(8), 1277 (1986).
21. H. Risken, *The Fokker-Planck Equation: Methods of Solution and Applications*, 3rd edition (Springer, 1996).
22. G. Osnabrugge, R. Horstmeyer, I. N. Papadopoulos, B. Judkewitz, and I. M. Vellekoop, "Generalized optical memory effect," Optica **4**(8), 886–892 (2017).
23. M. Marsan, M. Lucidi, and G. Cincotti, "LED-based spectrophotometry," *13th Pacific Rim Conference on Lasers and Electro-Optics (CLEO-PR)*, Hong Kong (2018).